Giant resonance study of ^{28}Si and ^{24}Mg with 240 MeV ^{6}Li scattering

X. Chen, Y. -W. Lui, H. L. Clark, Y. Tokimoto, and D. H. Youngblood

Inelastic scattering of ^{6}Li from both ^{28}Si and ^{24}Mg excited into the giant resonance region was measured with the spectrometer at 0° and 4° and at 6° for ^{24}Mg. The folding optical potential obtained with the CDM3Y5 NN interaction and with density **den1** (see Ref.[1]) were used to analyze the giant resonance data. Sample excitation energy spectra for ^{28}Si with average center of mass angles 1.3° and 6.4° are shown in Fig. 1 with pink curves representing the continuum choices. Angular distributions of the differential cross sections for the giant resonance peak and continuum are shown in Fig. 2 along with DWBA fits for three energy bins with average excitation energies 10.14 MeV, 20.46 MeV and 29.14 MeV. Sample excitation energy spectra for ^{24}Mg with average center of mass angles 1.3°, 4.7° and 9.5° are shown in Fig. 3 with pink curves representing the continuum choices. Angular distributions of differential cross sections for the giant resonance peak and continuum for ^{24}Mg are shown in Fig. 4 along with DWBA fits for three energy bins with average excitation energies 12.94 MeV, 20.08 MeV and 28.75 MeV.

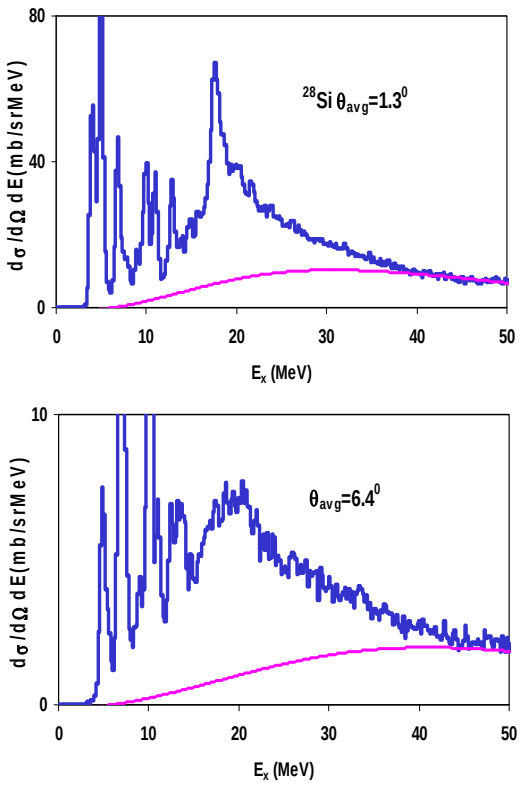

Figure 1. Sample spectra for ^{28}Si at average center of mass angle 1.3° and 6.4°. The pink curves are the continuum chosen for the analvsis.

The E0, E1, E2 and E3 strength distributions obtained for ^{28}Si are shown in Fig. 5 along with those obtained from α scattering. The multipole parameters obtained are summarized and compared with those from α scattering in Table I. The centroid (m_1/m_0), rms width and percentage of the EWSR are calculated for the total excitation range measured (~ 8 to 40 MeV), as well as the ranges ~ 8 to 22.4 MeV and ~ 22.4 to 40 MeV.

The E0, E1, E2 and E3 strength distributions obtained for ^{24}Mg are shown in Fig. 6 and Fig. 7 along with those obtained from two different analyses of α scattering. The multipole parameters obtained for ^{24}Mg are summarized and compared with those from α scattering and 156 MeV ^{6}Li scattering in Table II. The centroid (m_1/m_0), rms width and percentage of the EWSR are calculated for the total excitation range measured (~ 8 to 40 MeV), as well as for the range ~10 to 20 MeV.

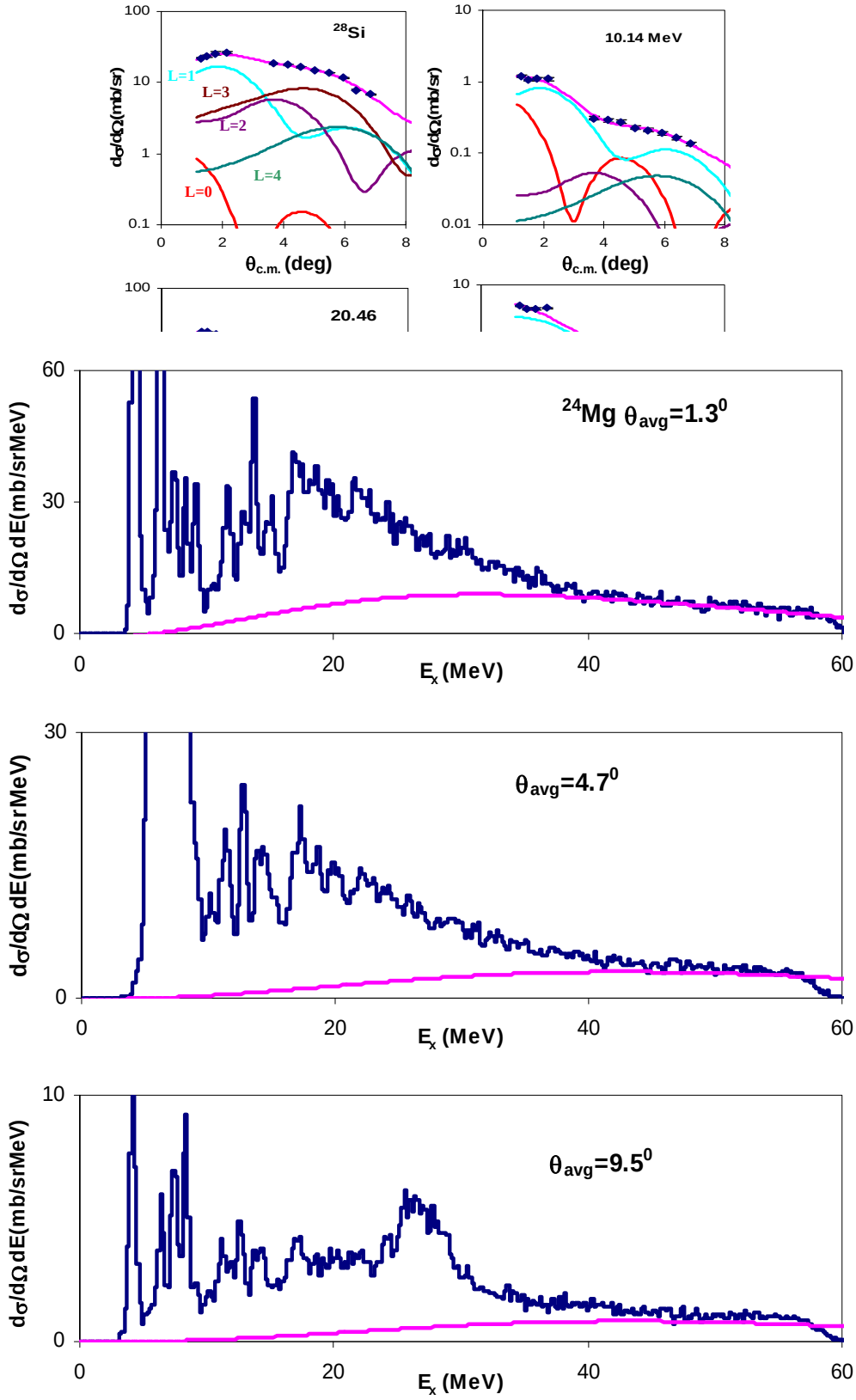

scatter y ^{6}Li
inelast Thus

Figure 3. Sample spectra for ^{24}Mg at average center of mass angle 1.3°, 4.7° and 9.5°. The pink curves are the continuum chosen for the analysis. The broad structures pointed by the brown arrow or covered by the brown bracket are from ^{6}Li scattering on Hydrogen.

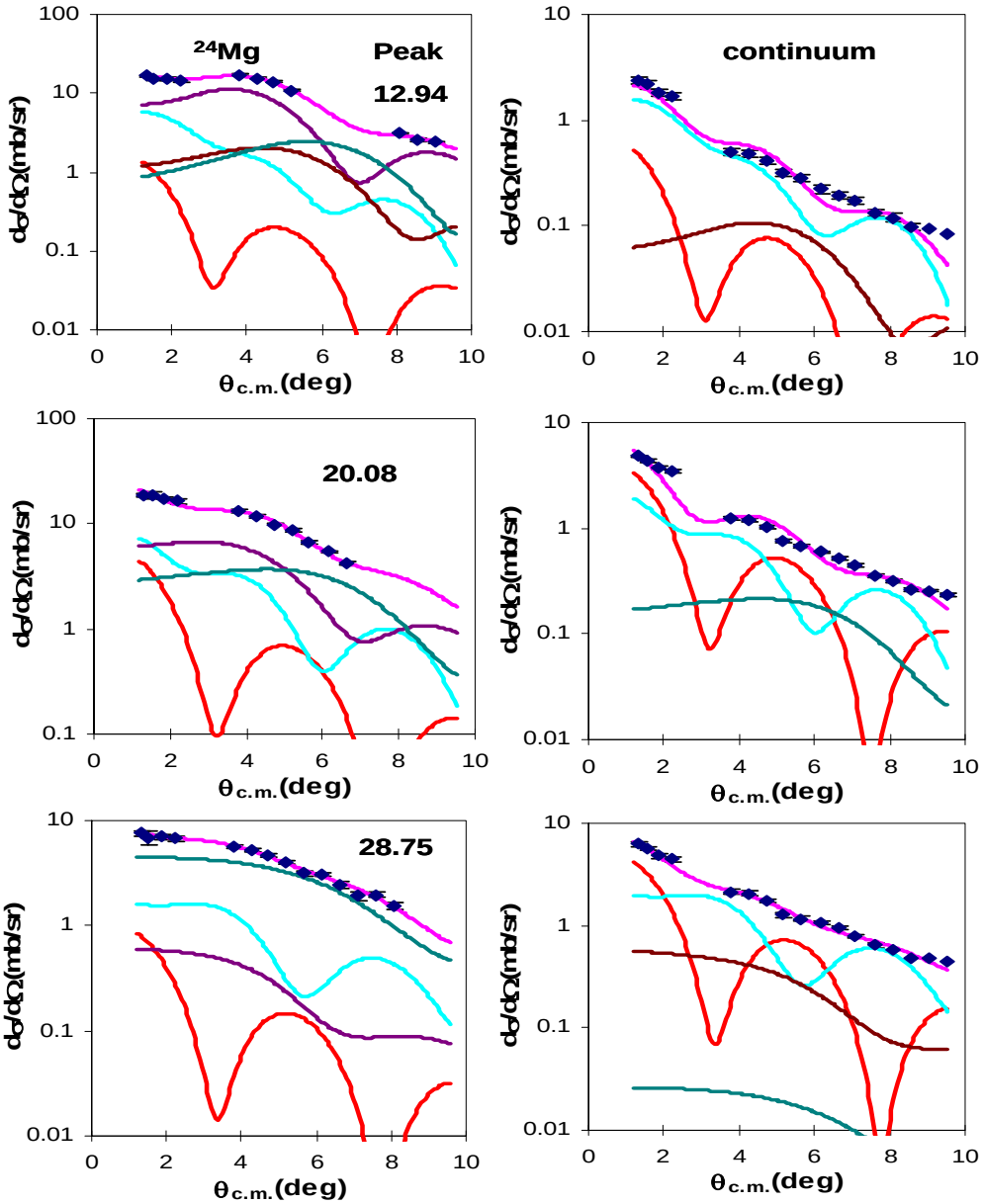

Figure 4. Angular distributions of the cross section for inelastic scattering from ^{24}Mg for 0.8 MeV wide bin centered at E_x=12.94, 20.08, 28.75 MeV along with DWBA fits. The left column shows those for the giant resonance peak while the right column shows those for the continuum. The pink lines through the data show the fits. The E0 contribution is shown by the red line, the isoscalar E1 contribution by the light blue line, the E2 contributions by the purple lines, the E3 contributions by the brown lines and E4 contributions by the dark green lines.

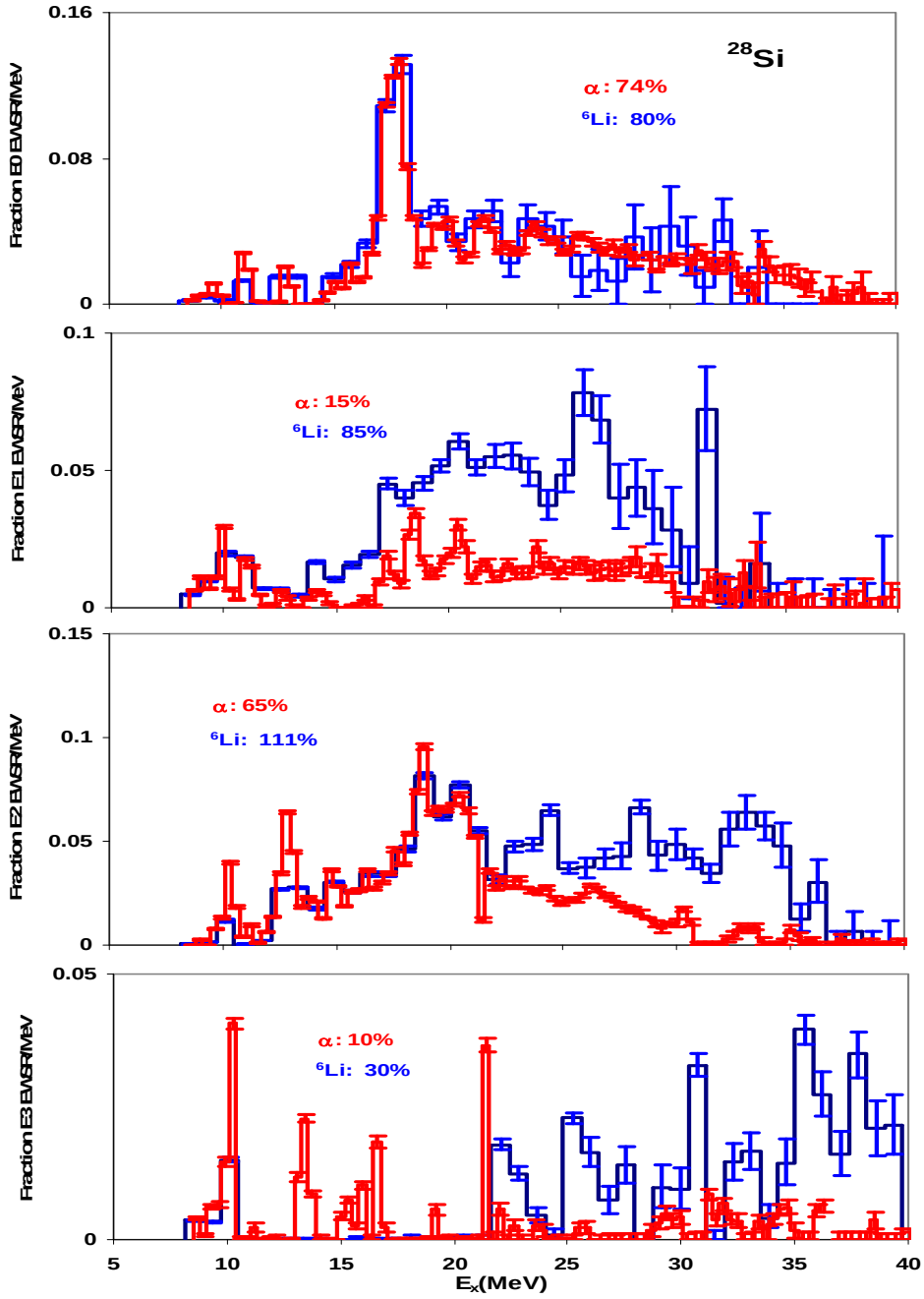

Figure 5. The dark blue curves show E0, E1, E2 and E3 strength distributions for ^{28}Si obtained from analysis of ^{6}Li inelastic scattering. The red curves show those obtained with α inelastic scattering [2]. Error bars represent the uncertainty due to the fitting of the angular distributions and different choices of the continuum.

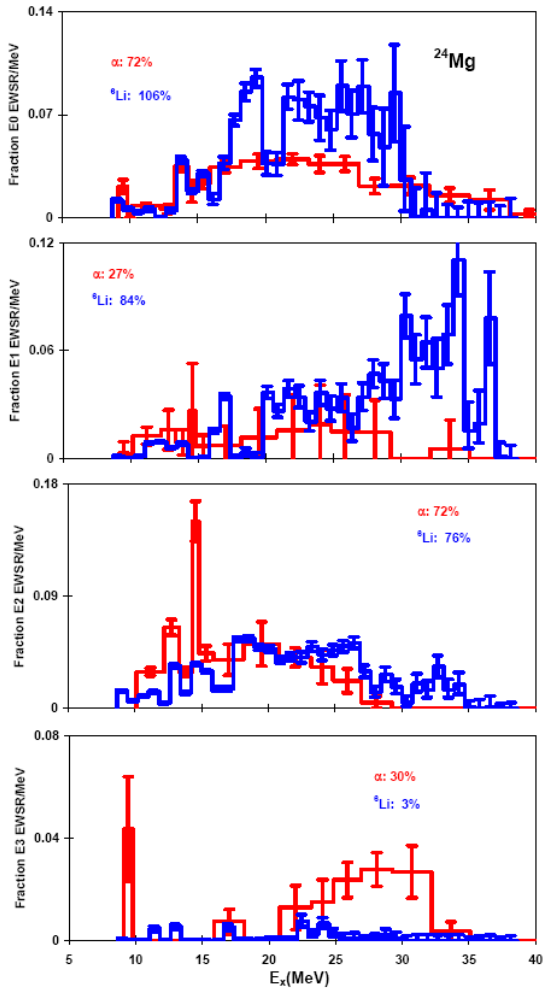

Figure 6. The blue curves show E0, E1, E2 and E3 strength distributions for ^{24}Mg obtained from analysis of ^{6}Li inelastic scattering. The red curves show those obtained with α inelastic scattering [3]. Error bars represent the uncertainty due to the fitting of the angular distributions and different choices of the continuum.

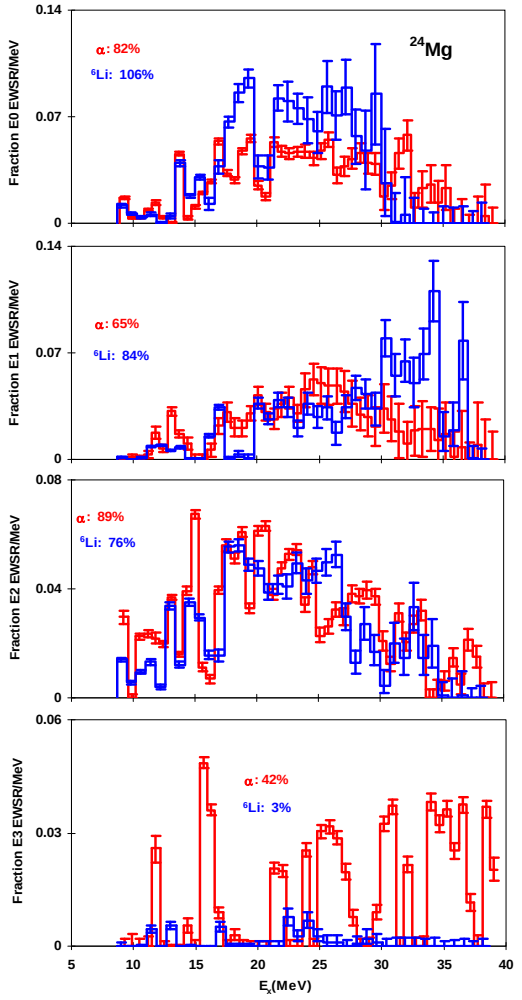

Figure 7. The blue curves show E0, E1, E2 and E3 strength distributions for ^{24}Mg obtained from analysis of ^{6}Li inelastic scattering. The red curves show those obtained with new analysis of α inelastic scattering [4]. Error bars represent the uncertainty due to the fitting of the angular distributions and different choices of the continuum.

Table I. Multipole parameters obtained for ^{28}Si in this work compared to those obtained from analysis of α scattering.

	This work				α scattering [2]			
	E_x range (MeV)	m_l/m_0 (MeV)	rms width (MeV)	EWSR (%)	E_x range (MeV)	m_l/m_0 (MeV)	rms width (MeV)	EWSR (%)
E0	8.0-22.4	17.60±0.17	2.67±0.17	48±6	8.0-22.5	17.27±0.38	3.04±0.6	38±4
	22.4-40.0	$27.72^{+0.73}_{-0.25}$	$3.21^{+1.34}_{-0.34}$	31^{+30}_{-13}	22.5-40.0	28.22±0.38	3.75±0.6	37±4
	8.0-40.0	$20.59^{+0.78}_{-0.33}$	$5.78^{+1.34}_{-0.34}$	80^{+35}_{-20}	8.0-40.0	$21.46^{+0.38}_{-0.38}$	6.3±0.6	74±10
E1	8.0-22.4	16.9±0.17	$3.77^{+0.74}_{-0.19}$	40±4	8.0-22.5	15.3±0.60	4.75±0.7	8±0.8
	22.4-40.0	$27.27^{+0.34}_{-0.20}$	$2.69^{+0.74}_{-0.19}$	38^{+19}_{-10}	22.5-40.0	27.56±0.60	3.05±0.7	7±0.7
	8.0-40.0	$21.17^{-0.41}_{-0.24}$	$5.87^{+0.74}_{-0.19}$	84^{+21}_{-11}	8.0-40.0	19.27±0.60	6.9±0.7	15±4
E2	8.0-22.4	17.25±0.17	3.02±0.23	47±5	8.0-22.5	16.59±0.25	3.5±0.6	47±5
	22.4-40.0	$29.22^{+0.20}_{-0.19}$	3.81±0.23	64±6	22.5-40.0	27.21±0.25	2.98±0.6	18±2
	8.0-40.0	$22.69^{+0.23}_{-0.20}$	6.94±0.23	111±16	8.0-40.0	18.53±0.25	4.7±0.6	65±9
E3	8.0-22.4	$12.94^{+0.25}_{-0.19}$	6.54±0.18	4^{+5}_{-1}	8.0-22.5	13.31±0.25	4.57±0.6	7±0.7
	22.4-40.0	32.15±0.17	4.48±0.18	27±3	22.5-40.0	33.32±0.25	3.48±0.6	3±0.3
	8.0-40.0	27.71±0.24	8.09±0.18	31^{+7}_{-6}	8.0-40.0	16.3±0.25	9.22±0.6	10±1

Table II. Multipole parameters obtained for ^{24}Mg in this work compared to those obtained from analysis of α scattering and from previous 156 MeV ^{6}Li scattering.

		^{6}Li scattering				**α scattering**				
L	Ref.	E_x energy (MeV)	m_l/m_0 (MeV)	rms width (MeV)	EWSR (%)	Ref.	E_x range (MeV)	m_l/m_0 (MeV)	rms width (MeV)	EWSR (%)
0	This work	10.2-20.6	$16.88^{+0.17}_{-0.17}$	2.13 ± 0.17	35±5	[3]	10.1-20.9	16.31±0.6*	2.62±0.74	27±4
		8.6-38.6	$21.35^{+0.37}_{-0.26}$	$4.98^{+0.68}_{-0.32}$	106^{+34}_{-24}		9.0-41.0	21.0±0.6	7.3±1.2	72±10
	[5]	10.0-20.2	16.66±0.5	2.48±0.5	34±3**	[4]	10.2-20.4	$16.44^{+0.33}_{-0.25}$	$2.48^{+0.48}_{-0.23}$	24±4
							9.0-41.0	$21.93^{+0.33}_{-0.25}$	$6.53^{+0.47}_{-0.23}$	82±9
1	This work	10.2-20.6	$14.75^{+0.20}_{-0.17}$	2.29 ± 0.17	10±3	[3]	10.1-20.9	14.68±2.21	3.14±0.97	12^{+11}_{-5}
							9.0-41.0	18.8±1.7	6.7±1.0	27^{+26}_{-11}
		8.6-38.6	$26.56^{+0.29}_{-0.26}$	$6.42^{+0.29}_{-0.27}$	84^{+24}_{-21}	[4]	10.2-20.4	$16.12^{+0.23}_{-0.20}$	$3.33^{+0.68}_{-0.49}$	16±5
							9.0-41.0	$22.70^{+0.23}_{-0.20}$	$6.19^{+0.67}_{-0.49}$	65±8
2	This work	10.2-20.6	15.79±0.17	2.58±0.17	30±4	[3]	10.1-20.9	15.07±0.6*	2.07±0.6*	51^{+5}_{-8}
							9.0-41.0	16.9±0.6	3.4±0.6	72±10
		8.6-38.6	$20.23^{+0.25}_{-0.20}$	$6.29^{+0.34}_{-0.25}$	76^{+14}_{-12}	[4]	10.2-20.4	15.56 ± 0.18	$2.93^{+0.25}_{-0.20}$	36±4
							9.0-41.0	$19.92^{+0.18}_{-0.18}$	$7.25^{+0.25}_{-0.20}$	89±9
3	This work	8.6-38.6	$18.54^{+1.40}_{-0.38}$	$5.85^{+0.28}_{-0.19}$	3^{+4}_{-1}	[3]	9.0-41.0	25.2±1.0	4.5±1.2	31^{+9}_{-6}
						[4]	9.0-41.0	$25.43^{+0.37}_{-0.23}$	$8.31^{+0.23}_{-0.22}$	42±5

* assume the uncertainty is the same as in the total energy range

** The original result from Ref. [5] multiplied by 0.5 (see Ref. [3])

[1] X. Chen, Y. -W. Lui, H. L. Clark *et al.*, *Progress in Research*, Cyclotron Institute, Texas A&M University (2006-2007), p. I-15
[2] D. H. Youngblood, Y. -W. Lui, and H. L. Clark, Phys. Rev. C **65**, 034302 (2002).
[3] D. H. Youngblood, Y. -W. Lui, and H. L. Clark, Phys. Rev. C **60**, 014304 (1999).
[4] D. H. Youngblood (private communication).
[5] H. Dennert, E. Aschenauer, W. Eyrich, *et al.*, Phys. Rev. C **52**, 3195 (1995).